Physics of pion production for a neutrino factory and a muon collider

Jarosław Pasternak

Institute of Theoretical Physics, Wrocław University

written at

Institut des Sciences Nucléaires, Université Joseph Fourier de Grenoble

Abstract

Intense muon beams are needed for new generation neutrino oscillations experiments , beyond the present long base-line projects and for a muon collider. A detailed knowledge of pion production processes in proton - nucleus collisions is important for the optimization of a pion collection. A motivation for neutrino physics are reviewed and essence of oscillation phenomenon is presented. Overview of technical aspects of neutrino factory and muon collider is given. Then physical conditions for pion production in proton-nucleus collisions are studied. Comparison of simulations at low proton kinetic energy (2 GeV) using different codes is presented. Physical considerations underlying the models are discussed. Results from simulations for thick Hg target are reviewed. Some conclusions for construction of a pion collector are given. A short introduction to quantum transport theories is presented.

Contents

Acknowledgments

To Tadeusz

1 Introduction

Neutrino is one of the most interesting and simultaneously mysterious elementary particle in modern physics. In particular a possibility of existence of neutrino oscillations strongly suggested by athmospheric SuperKamiokande experiment increased an activity in this field of physics both in experiment and theory. In the Standard Model neutrino is massless lefthanded neutral particle with spin 1/2, which participate only in weak interactions. A lack of a righthanded neutrino is dictated by results of experiments, which never detected this particle. But apriori there is no reason for massless neutrino like for example for photon, where its masslessness is explained by gauge invariance. To give a mass to neutrino in the Standard Model using the Higgs mechanism in the same way like for other fermions, one has to introduce righthanded neutrinos, which interact only with Higgs boson and in gravitational way. If neutrino has a mass it can behave in weak interaction in a similar way like quarks; states participating in weak interaction need not be mass eigenstates. One can introduce a mixing matrix U for neutrinos in analogy to Cabibbo-Kobayashi-Maskawa matrix for quarks, which is not expected to be diagonal:

$$|\nu_f> = \sum_m U_{fm}|\nu_m>, \tag{1}$$

where $|\nu_f>$ are flavor eigenstate, which interact weakly and $|\nu_m>$ enter the Higgs mechanism. Neutrinos are produced and detected in weak interactions, but their propagation is governed by mass eigenstates. Therefore one can observed the oscillation phenomenon, in which neutrino produced in one flavor reaches a detector in another one. The time dependence of a state can be described by:

$$|\nu_f(t)> = \sum_m e^{-iE_m t} U_{fm}|\nu_m> . \tag{2}$$

Than an amplitude to find another flavor state in a beam is, using an orthogonality of mass eigenstates:

$$<\nu_g|\nu_f(t)> = \sum_m e^{-iE_m t} U_{fm} U_{gm}^* \tag{3}$$

The probability of this process is given by a formula:

$$P(f \to g) = \sum_m |U_{fm}^*|^2 |U_{gm}|^2 + 2Re[\sum_{m \neq n} U_{fm}^* U_{gm} U_{fn} U_{gn}^* cos(\frac{\delta m_{mn}^2 t}{2p})], \tag{4}$$

where the ultrarelativistic approximation was used:

$$E_m \simeq p_m + \frac{m_m^2}{2p_m}. \tag{5}$$

It is also assumed that:

$$p_m \simeq p_n. \tag{6}$$

and δm_{mn}^2 in equation (4) is given by:

$$\delta m_{mn}^2 = m_m^2 - m_n^2. \tag{7}$$

After defining the distance at which the argument of $cos(\frac{\delta m_{mn}^2 t}{2E})$ becomes 2π - the so called oscillation length:

$$L = \frac{4\pi E}{\delta m_{mn}^2} \qquad (8)$$

and taking into acount the 2 generation case (without CP violation) with the mixing matrix:

$$\begin{pmatrix} cos\theta & sin\theta \\ -sin\theta & cos\theta \end{pmatrix}, \qquad (9)$$

finally we can get a formula for oscillations:

$$P(f \to g) = sin^2(2\theta)sin^2(\frac{\pi x}{L}), \qquad (10)$$

where a time was replaced by the distance x covered by the beam. From the last formula we can see that a possibility of observation the oscillation phenomenon is sensitive to the distance from the source to detector and to energy of neutrinos. The neutrino detection is realized by neutrino interaction, which is very weak and proportional to energy so we cannot observe a very low energy neutrino. Using higher energy, we have chances for a measurement but in order to see oscillation we have to take longer distances (oscillatory behavior becomes prominent when $x \sim L$).

One can use natural sources of neutrinos: the Sun or atmosphere under influence of cosmic rays, but several uncertainties in a Sun model or an atmospheric neutrino flux make predictions very difficult. People use also neutrinos coming from nuclear reactors or so called accelerator ones, which come from production of neutrinos from decaying accelerated particles. The last case seems to be particulary interesting, because of possibility of making a very intense neutrino beam with very good parameters. A good example is the K2K experiment, which uses a muon neutrino beam coming from pion decays. Layout of the K2K experimental area is shown on figure 1. The experiment is constructed in the following way: proton beam with kinetic energy 12 GeV hits the aluminium target, where several kinds of particles are produced in proton-nucleus collisions, mostly pions of both charges. Pions reach decay channel, where positive pions are accelerated by system of two magnetic horns (see figure 2).

Then they decay into positive muons with lifetime $2.6 \times 10^{-8} s$ and muon neutrinos:

$$\pi^+ \to \mu^+ + \nu_\mu$$

Muons are stopped in the matter, but neutrinos reach the first detector located after muon stopping and then travel a distance of about 200 km to SuperKamiokande detector (see figure 3).To increase the potential of measurement in a long baseline experiments people want to go step further and prepare a muon beam, based on muons, which are lost in K2K experiment. Muons after acceleration and cooling can be used to create a neutrino beam via a reaction:

$$\mu^{+(-)} \to e^{+(-)} + \nu_e(\bar{\nu}_e) + \bar{\nu}_\mu(\nu_\mu)$$

in the neutrino factory or can be further accelerated in muon collider, which gives a very good opportunities for testing high energy physics and can stay a future for high energy colliders.
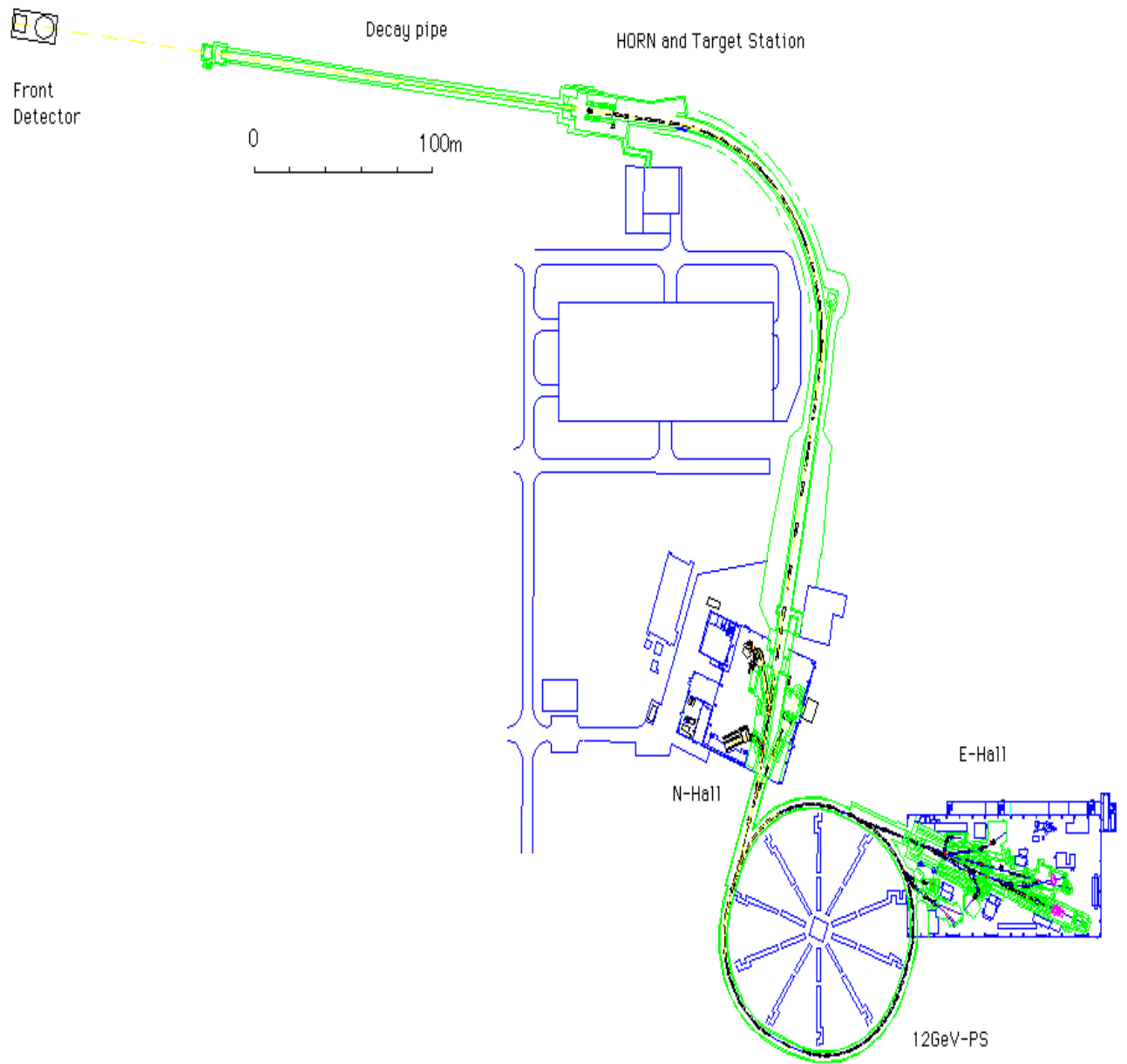
Decay pipe

HORN and Target Station

Front
Detector

0   100m

E-Hall

N-Hall

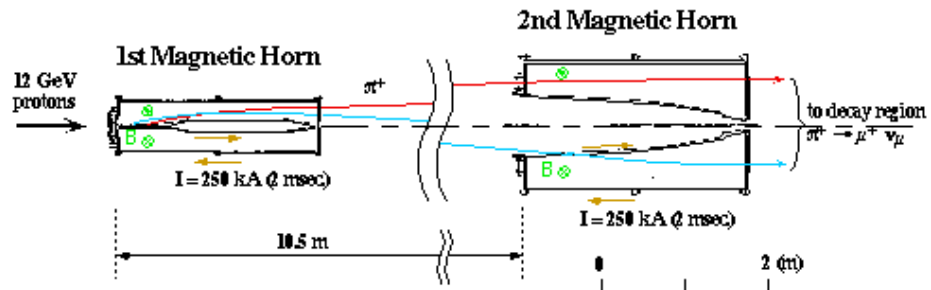12GeV-PS

Figure 1: Layout of the K2K experimental area

Figure 2: Magnetic horns system in the K2K

The oscillation phenomenon can be easily understood, as a beautiful quantum process, but the origin of a neutrino mass remains to be a great secret for a theory. It seems, that some extension of the standard model is necessary in order to incorporate massive neutrinos. Even a nature of this particle (Dirac or Majorana) is not known. Let me remind, that Dirac particle is described by four component Dirac spinor, two components for particle and two for antiparticle, which are different species. Majorana particle can be described only by two components, because particle and antiparticle are the same species. The most general mass term of fermionic lagrangian is given by:

$$\mathcal{L} = \frac{1}{2}(\bar{\nu}_L \bar{\chi}_L^c) \begin{pmatrix} M_L & M_D \\ (M_D)^T & M_R \end{pmatrix} \begin{pmatrix} \nu_R^c \\ \chi_R \end{pmatrix} + h.c., \tag{11}$$

where $\nu = (\nu_e, \nu_\mu, \nu_\tau, ...)$ are active neutrinos - (from LEP Z^0 decay data we know, that there exist 3 such neutrinos with mass less than 45 GeV), $\chi = (\chi_1, ..., \chi_{n_s})$ are "sterile" righthanded neutrinos, which has no electroweak couplings. In this case M_L is 3×3 lefthanded Majorana mass matrix, M_R is a $n_s \times n_s$ righthanded Majorana mass matrix and M_D is 3-row by n_s-column Dirac mass matrix. The number n_s of "sterile" neutrinos depends on a specific model. In the standard model, minimal supersymmetric standard model or minimal SU(5) grand unified theory (GUT), $n_s = 0$, while in the SO(10) GUT, $n_s = 3$. An explanation for three known ultra-light neutrino masses could be provided by so called seesaw mechanism, which connects two mass scales:

$$m_\nu = \frac{m_D^2}{m_R}, \tag{12}$$

where m_D is a mass scale of the standard model (quarks mass) and m_R is a mass scale of GUT ($10^{15} GeV$). Neutrino physics is an interesting subject [1,2] for a theory and for an experiment, because it enables to ask a fundamental questions and to verify it experimentally.

2   Technical aspects of a neutrino factory

Neutrino beams play a very impotant role in modern physics. They were used to show a difference between muon and electron neutrinos, with their help neutral current interactions were discovered. Neutrino beam can be used also to test deep inelastic interactions in neutrino nucleon reactions or for precise tests of electroweak physics. As was mentioned in the previous chapter it allows to ask fundamental questions via neutrino oscillation phenomenon. As a conventional accelerator neutrino beam one understands neutrinos created in decays of mesons: pions and kaons. This is mostly a muon neutrino beam with a small fraction of electron neutrinos via three body kaon decay $K^+ \rightarrow e^+ \pi^0 \nu_e$. Antyneutrinos can be created using mesons of opposite charge. Using a very high energy proton beam a small component of tau neutrinos can be obtained, coming predominantly from prompt taonic decays of D mesons. This kind of beam composition is not the best one for searching for the oscillation phenomenon. For example a big uncertainty in ratio of muon and electron neutrinos introduces systematic error for many neutrino experiments. Also looking for $\nu_e \rightarrow \nu_\mu$ or any other flavor or sterile neutrinos is not possible, because of a small fraction of electron neutrinos in the beam.
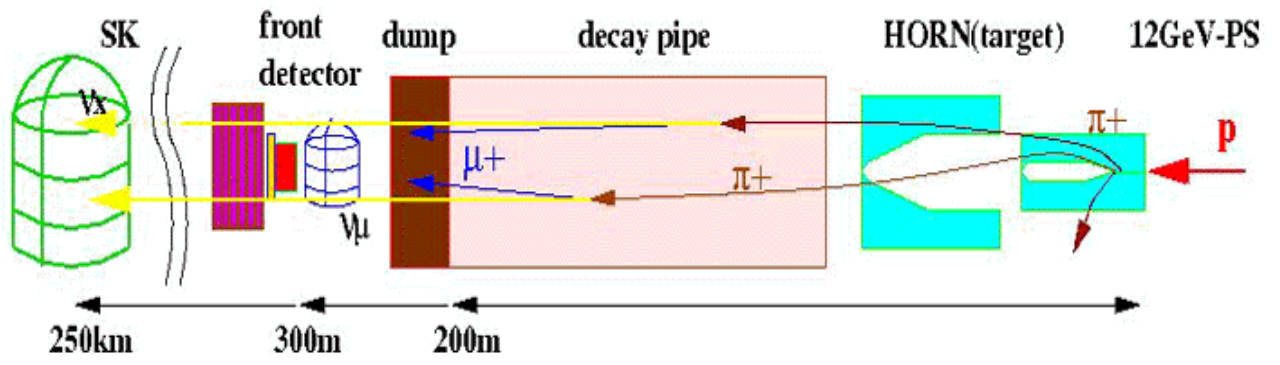
Figure 3: Neutrino beamline in the K2K.

8

In a neutrino beam coming from muon decay equal fractions of muon neutrinos and electron antineutrinos can be achieved from μ^- and muon antyneutrinos and electron neutrinos from μ^+. Also muon lifetime is about 100 times longer than lifetime of charged pion. This enable a precise preparation of a beam, including focusing and acceleration. Even a polariztion of muons can be applied to increase a measurement potential. A difference in lifetime makes conventional decay channels constructed for mesons too short for muons. For ilustrative exemple, muons accelerated to momentum 20 GeV/c have a decay length $\gamma c\tau = 126 km$. This problem can be solved using a recirculation system with a straight section pointed in a direction of detector. Muons moving in such a storage ring spend much time in this straight section decaying into neutrinos [3]. The possibility of a neutrino factory based on a muon storage ring has received much attention. Now I would like to describe shortly building blocks of the neutrino factory [4]. The first step is a proton machine, which should accelerate protons to laboratory kinetic energy of a range $10^0 - 10^2$ GeV according to designed project with a high intensity simultaneusly. The most important parameter is a power of the machine, which is a product of energy and intensity. In many studies of the neutrino factory there appears a concept of 4 MW proton beam. For proton beam 2 GeV kinetic energy, it means approximately 1.24×10^{16} particles per second (particles are in fact accelerated in pulses according to some frequency, which is another parameter of an accelerator). In some projects special accumulators ware proposed for protons to give to a beam time structure compatible for a decay of the muons in the decay ring or to assure a proper pressure conditions on a target. The next step is a target section. Here the most popular concept is to use a cylidrical target of a length of order of interaction length and a radius of order 1 cm placed in a high magnetic field selenoid.

An average interaction length λ is a specific quantity that characterizes inelastic processes, which describes inelastic interaction of hadrons in matter according to exponential law:

$$N = N_0 e^{-\frac{x}{\lambda}}, \tag{13}$$

where x is a target thickness. λ can be calculated as follows:

$$\lambda = \frac{A}{N_A \varrho \sigma_{inel}}, \tag{14}$$

where A is atomic mass in g/mol, N_A is the Avogadro number in mol^{-1}, ϱ is a density in g/cm^3, and the inelastic part of hadronic cross section σ_{inel} is in cm^2. (It is in general energy dependent, but increases very slow at high energy. Here its constant value is used only for estimations and values for several materials can be found in [25].) For a particular case of mercury λ is 13 cm. This quantity describes a mean free path of hadrons in some material between inelastic interactions.

The idea to keep produced particles in a magnetic field is due to simple observation, that charged particles move in magnetic field along a circular orbit with radius defined by a field and transvers momentum p_t:

$$R = \frac{p_t}{eB}. \tag{15}$$

If target radius is shorter than an internal radius of the selenoid, most of pions up to p_t will be transported in this system. The target selenoid is followed by a transport selenoid where the field is adiabatically reduced, while the radius is increased. In this channel pions decay

into muons, which increases a transvers phase space. I will come back to this problem in the chapter 3. For acceptance of pions, p_t limit plays an important role, but is not the only one. The second one is a cut in longitudinal component coming from RF system, which is indispensable for particle acceleration. Also the particles cannot be to slow because of a fast decay of pions and also coming from it muons. This limit is treated differently in several projects, for example rapidity cut between 1 and 2 can be found. Definition of rapidity is as follows:

$$y = arctanh(\frac{p_z}{E}), \tag{16}$$

where z axis is taken along the proton beam line.

There is also a serious problem with energy, which will be deposited in the target (up to about 10%). A thermal radiation is insufficient as cooling and a thermal bath can absorb too many particles. A moving target is proposed to be cooled according to external heat exchanger. In this project both solid and liquid target materials can be applied. In particular liquid mercury jet target is discussed with a lot of hope. After the target section the decay (transport) selenoid is placed. To create a muon beam with good parameters cooling of muons is needed. I will discuss it in the next chapter. After the cooling and acceleleration of muons, they reach the decay ring, which is constructed to send neutrino beams to detectors, firstly to the near detector just after the decay channel and secondly to the far detector, which can be placed in a distance of order $10^1 - 10^3$km. For the time being a discussion about geographical locations of both the accelerator site and the far detector is still open to very interesting speculation.

3   Muon collider, beam emittance and muon cooling

High energy accelerators used to explore fundamental laws of the nature are big and expensive machines. To produce high energy collision, where new particle states can be seen, electron-positron or proton collision are used for example in the LEP (CERN) or in the TEVATRON. The LHC project is under construction and will be started in 2005 in CERN. It will be a 27.6 km in circumsterence proton-proton collider with 14 TeV energy in the center of mass and luminosity $10^{34}cm^{-2}s^{-1}$. It will offer a good opportunity to make fundamental discoveries. But to move one order of magnitude higher in energy seems to be extremaly difficult using present approches. It is because of several reasons. Firstly hadrons are composed from quarks, so an effective energy for new particle production is lower , then a real one. On the other hand electron-positon collider is limited by energy loss in synchrotron radiation and bremstrahlung effects, which increase as $(E/m)^4$. These difficulties can be overcome using a heavier kind of electrons - muons, which are also point-like species, but being about 200 times heavier, than electrons have negligible radiation effects [5,6]. Good motivation for a muon collider could be a unique opportunity for discovery and factory-like production of Higgs bosons in the s-channel [7], which if exist, would be discovered firstly at the LHC. Also supersymmetric particles could be seen in $\mu^+\mu^-$ collider with multi TeV collision energy, if a supersymmetry breaking scale is of order 1-2 TeV [8]. The most important problems of muon collider are the following: firstly muons are unstable particles and secondly they are created into a very large phase space. The lifetime of muon is sufficient to make a storage ring collisions after acceleration and the phase space can be reduced by an ionization cooling.
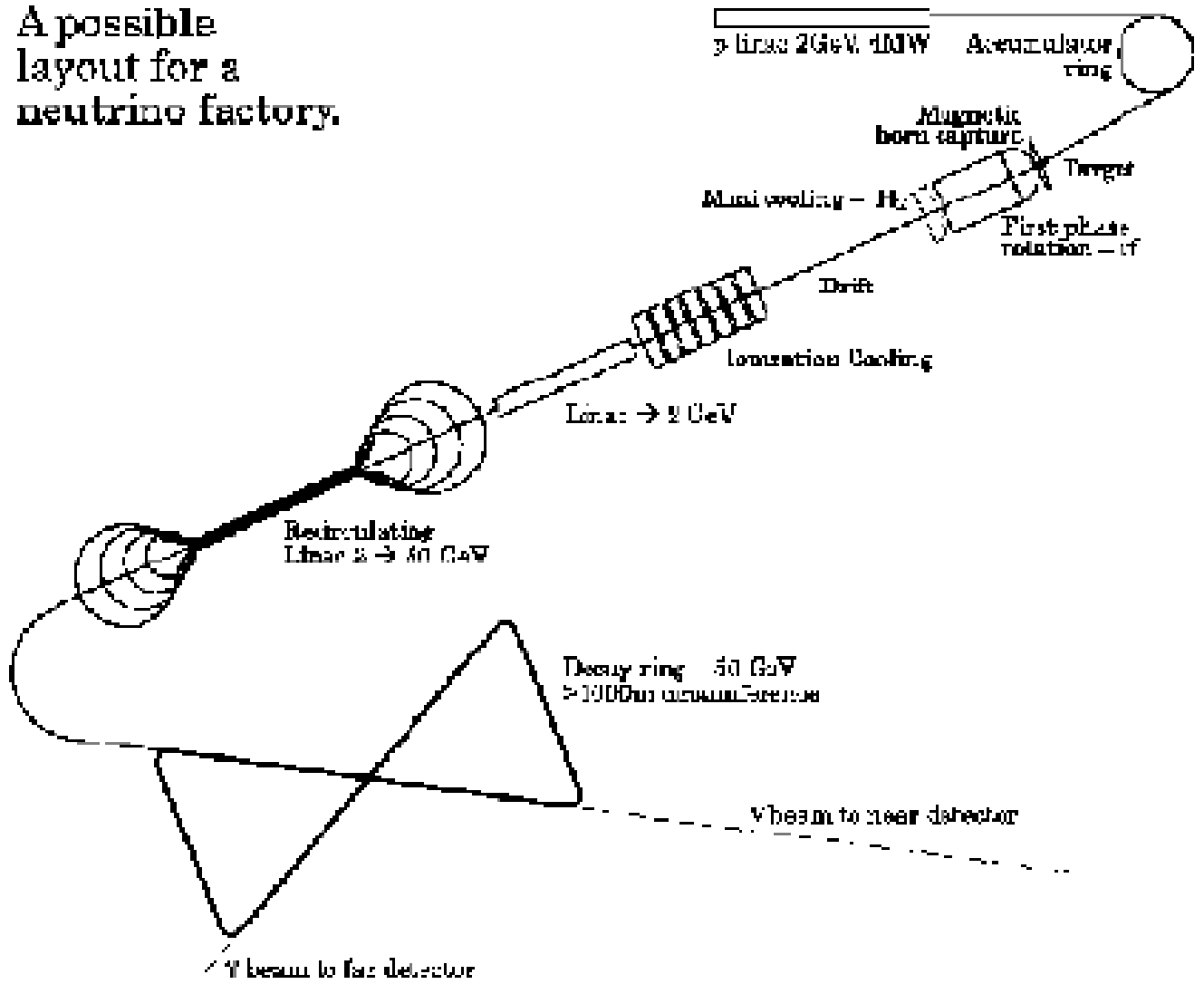
A possible
layout for a
neutrino factory.

p-linac 2GeV 4MW   Accumulator
                    ring

                    Magnetic
                    horn capture
Mini cooling — H₂   Target
                    First phase
                    rotation — rf

                    Drift

              Ionization Cooling

              Linac → 2 GeV

Recirculating
Linac 2 → 50 GeV

              Decay ring   50 GeV
              >1000m circumference

              ν beam to near detector

ν beam to far detector

Figure 4: Prototype of the neutrino factory.
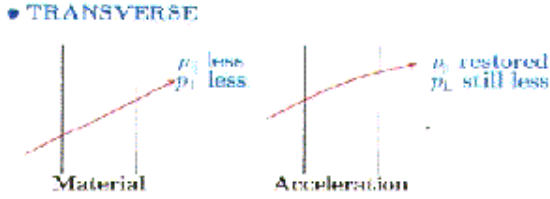
IONIZATION COOLING

● TRANSVERSE

Figure 5: The idea of an ionization cooling.

I would like to explain a definition of emmitance of a particle beam and its reduction, which is called cooling. The emittance is connected with a volume in the six dimensional phase space with three position coordinates (x,y,z) and three momentum coordinates (p_x, p_y, p_z). This space can be factorized into two sub-spaces: transverse and longitudinal one according to the beam direction. One usualy defines a transverse emittance in a trace space [9], which is a little modified version of transverse phase space: it is expressed in terms of the position - x and the transverse angle $\acute{x} = dx/dz$. The relation between trace space and phase space is given by:

$$p_x = \acute{x} p_z. \tag{17}$$

The emittance is defined as an area of the elipse in a trace space containing the beam, divided by π:

$$\varepsilon_x = \int dx d\acute{x} / \pi [m \times rad]. \tag{18}$$

During an acceleration the volume in the trace space is reduced via decreasing of $\acute{x}$. The transverse momentum is related to the inclination angles via:

$$p_x = \acute{x}(\beta\gamma)(m_0 c). \tag{19}$$

Defining the so called normalized emittance as volume in a modified trace space $(x, \beta\gamma\acute{x})$ one can have a conserved quantity. From the Liouville theorem it is known, that the phase space volume is a conserved quantity for Hamilton systems. But in a real situation this quantity is not conserved due to existence of a dissipative systems, internal degrees of freedom or energy exchange with other system. In particular it can be used to reduce the emittance to make parameters of the beam better for particular applications.

In the case of neutrino factory or muon collider pions are created in a very big phase space volume and pion decays only increase it. To achieve a muon beam, which can be focused and accelerated for experimental applications, its phase space has to be reduced. Actually existing cooling methods seem to be not efficient for muon beams. For example synchrotron radiation cannot be used because of big muon mass. A solution of this problem can be provided by so called ionization cooling. The simple idea is explained by the following consideration: a muon beam traverse an absorber with a very big interaction length (due to collisions with a nuclei). In the absorber two phenomena take place. Energy is lost by ionization in interaction with electrons, which reduce momentum of muons. Collisions with nuclei can change a direction of a muon motion. The first process makes cooling

and the second one heating. Balancing between two processes is possible taking a medium with big interaction length like liquid hydrogen. Muons leaving an absorber are accelerated in the longitudinal direction. A netto result is a reduction of the transverse phase space according to decreasing of the total momentum in medium and then increasing only its longitudinal component. It does not break Liouville theorem, because it takes place in a dissipative system. It seems, that muon collider is a very promising idea for future high energy colliders. Its technological problems can be overcome just in a neutrino factory, which could be a steping stone for a muon collider. An activity in this field is increasing and several kind of experiments were proposed or even accepted to run in a near future.

4   Description of pion and its interaction

The existence of a pion was postulated by Yukawa in 1935 to explain a finite range of nuclear interaction. Creation of a virtual particle with a mass m implies "violation" of energy conservation in a time interval described by uncertainty principle $\Delta t <= \hbar/mc^2$. In this time the particle can move on a distance $R < c\Delta t <= \hbar/mc$. It shows, that associating an interaction with a quanta of a field - a massive particle being exchanged we can achieve a finiteness of an interaction range. Taking the relativistic Klein - Gordon equation and applying it to a static case we can neglect a time derivative:

$$\nabla^2 U(r) = \frac{1}{r^2}\frac{\partial}{\partial r}(r^2\frac{\partial U}{\partial r}) = \frac{m^2 c^2}{\hbar^2}U(r) \tag{20}$$

The solution of this equation can be treated as a nuclear potential between nucleons carried by pions. Decreasing nature of this Yukawa potential reflects a finiteness of an interaction range:

$$U(r) = \frac{g}{r}e^{-r/R}, \tag{21}$$

where $r = \frac{\hbar}{mc}$ and g can be identified as a coupling constant. Firstly muon was thought to be a Yukawa particle, but it was observed that it doesn't participate in strong interactions. In 1947 pions were observed in cosmic rays showers on a photographic emulsion.

Pion is a spinless particle, which participates in every kind of interaction. It is a hadron existing in Nature in three charge states π^+, π^-, π^0. The mass for charged pion is 139.56995 ± 0.00035 MeV and for the neutral one 134.9764 ± 0.0006 MeV. It is convenient to introduce an isospin formalism in analogy to spin system. Nucleon is treated to be a particle with two possible states- proton and neutron like a 1/2 spin particle, with two possible spin orientation "up" and "down". It is because proton and neutron behave in the similar way in strong interactions. It is postulated that isospin commutes with Hamiltonian of strong interactions, so it is a conserved quantity. Proton and neutron states can be described in this formalism in the following way:

$$|p> = \begin{pmatrix} 1 \\ 0 \end{pmatrix} \tag{22}$$

$$|n> = \begin{pmatrix} 0 \\ 1 \end{pmatrix} \tag{23}$$

Thus these states are eigenstates of τ_3 operator being a z-component of isospin operator. Proton has $t_z = +\frac{1}{2}$ and neutron $t_z = -\frac{1}{2}$. Introducing a baryon number B for nucleon equal to 1, one can deduce a relation between a charge, isospin and baryon number:

$$Q = t_z + \frac{1}{2}B \qquad (24)$$

Assuming this relation to be valid for pions with baryon number equal zero, we can see that thay have to be an isospin triplet. Raising and lowering operators can be constructed like in the spin formalism. The "direction" of an isospin has to be understood in an abstract way in "isospin space". The action of raising and lowering operators $\tau_\pm = \frac{1}{2}(\tau_1 \pm i\tau_2)$ change states:

$$\tau_+ |n> = |p> \qquad (25)$$

$$\tau_- |p> = |n> \qquad (26)$$

From a quark model we know, that wave functions of nucleons can be represented by product of up and down quark wave functions:

$$|p> = |uud> \qquad (27)$$

$$|n> = |udd> \qquad (28)$$

Action of isospin raising and lowering operators on nucleon states can be understood as changing u quark into d and vice versa. The conclusion can be made that u and d quark form an isospin dublet. Taking into account that third isospin component is opposite for particles and antiparticles, what can be seen from $p\bar{p} \to \gamma\gamma$, we can try to predict quark structure of pions:

$$|\pi^-> = |\bar{u}d> \qquad (29)$$

Than application of rising operators to quark states produced π^0 and π^+ states:

$$|\pi^0> = \frac{1}{\sqrt{2}}(|u\bar{u}> - |d\bar{d}>) \qquad (30)$$

$$|\pi^+> = -|u\bar{d}> \qquad (31)$$

This simple model describes nucleons and pions only approximately. Presently accepted theory of strong interactions is the QCD - a nonabelian gauge field theory, which contains as fundamental fields quarks and gluons as mediating gauge bosons. In this theory baryons and mesons are bounds states of quarks and gluons surrounded by a see of virtual quark and gluon states creating and annihilating in a vacuum in such a way that free quarks and gluons can be deconfined in a very high energy heavy ions collisions with energy of 156 GeV/A (per nucleon) creating a new state of matter: quark-gluon plasma. At lower energy quarks and gluons are confined in baryon and meson species. Unfortunately QCD calculations cannot be applied in low energy reactions of hadrons. It is because our formalism of quantum field theory is suitable for making a summation of series of Feynman graphs, which are power series in a coupling constant. If a theory is renormalizable and the coupling constant is small, it is enough to add first few terms to have a result, which is comparable with an experiment. This is a case for the QED and electroweak theory, but not with QCD

where the situation is more complicated. The coupling constant is much bigger, than in electrodynamics, so perturbative series cannot be convergent. Perturbative QCD may be useful because of so called asymptotic freedom - a coupling constant is decreasing to zero for higher energy. One can start to apply p-QCD from an energy range 10^1 GeV and it can be fully used in deep inelastic scattering for 10^2 GeV. But for lower energies we can only use some phenomenological approch based on conservation laws, asymptotic behavior, unitarity of S matrix etc. We can start treating species as pointlike objects and try to introduce some methodes known in other fields. Firstly we assume that pointlike pions and nucleons satisfied the Dirac and Klein-Gordon equations respectively. Then taking into account a negative parity of pion we try to construct a pseudoscalar interaction Lagrangian [10]:

$$\mathcal{L}_{PS} = -g\bar{\Psi} i\gamma_5 \tau \Psi \phi, \tag{32}$$

and pseudovector interaction Lagrangian:

$$\mathcal{L}_{PV} = \frac{f}{m_\pi} \bar{\Psi} \gamma^\mu \gamma_5 \tau \Psi \partial_\mu \phi \tag{33}$$

It can be shown by partial differentiation and application of Dirac equation that this components are equivalent. Then one can make a nonrelativistic approximation and apply it to low energy reactions together with partial waves decomposition of wave function. The direct use of a field theory with such Lagrangian at higher energy is impossible, because with increasing energy other particles began to play important role in strong interactions and the last Lagrangian is not complete. Taking into consideration nucleons, pions, delta resonance P(3,3) which can interact with exchange of virtual σ, ω, π and ρ mesons our Lagrangian (a free part) looks like so called QHD (quantum hadronodynamics) [11]:

$$\mathcal{L}_F = \bar{\Psi}(i\gamma_\mu \partial^\mu - M_N) + \bar{\Psi}_{\Delta\nu}(i\gamma_\mu \partial^\mu - M_\Delta)\Psi_\Delta^\nu + \frac{1}{2}(\partial_\mu \pi \partial^\mu \pi - m_\pi^2 \pi^2) + \frac{1}{2}(\partial_\mu \sigma \partial^\mu \sigma - m_\sigma^2 \sigma^2)$$

$$-\frac{1}{4}\omega_{\mu\nu}\omega^{\mu\nu} + \frac{1}{2}m_\omega^2 \omega_\mu \omega^\mu - \frac{1}{4}\rho_{\mu\nu}\rho^{\mu\nu} + \frac{1}{2}m_\rho^2 \rho_\mu \rho^\mu + s.i. \tag{34}$$

where tensor $\omega_{\mu\nu} = \partial_\mu \omega_\nu - \partial_\nu \omega_{mu}$ and similar for $\rho_{\mu\nu}$ and s.i. means a self interaction component. Here ω and ρ vector mesons are real hadronic species playing an important role in attractive short range part of nucleon-nucleon interactions, but σ is an effective degree of freedom, which can be identified as a double pion exchange. This suggest that even here because of very complicated calculations and quite big coupling constants only a first order Born approximation can be done.

During last years there appeared another approach using so called effective field theory. Here it is assumed that below certain energy scale, all heavy degrees of freedom are not present in interactions. Technically speaking we can omit some parts of Lagrangian taking only light particles. It enables to use the perturbation theory again. A new effective theory takes symmetry principles from a fundamental one. A good example is an application of this scenario to QCD in the so called chiral perturbation theory, which takes its name from chiral symmetry $SU(N_f)_L \times SU(N_f)_R$ comeing from QCD. Here N_f denotes the number of quark flavors (u, d, s, c, b, t) taking part in a theory. For example N_f=2 theory contain only u and d quark. The chiral symmetry is an approximately spontaneusly broken global symmetry,

what suggests an existence of massless Goldstone bosons. Pion is a good candidate for such a particle with mass much less than nucleon (existence of nonzero pion mass means that chiral symmtery is not an exact symmetry). At low energies QCD Lagrangian can be replaced by an effective Lagrangian, which with pions alone has a form:

$$\mathcal{L} = \frac{F^2}{4} Tr(\partial_\mu U \partial^\mu U^\dagger + M^2(U + U^\dagger)), \tag{35}$$

where:

$$U = \sigma + \frac{i\phi}{F}, \tag{36}$$

$$\phi = \begin{pmatrix} \pi^0 & \sqrt{2}\pi^+ \\ \sqrt{2}\pi^- & -\pi^0 \end{pmatrix}, \tag{37}$$

$$\sigma = [1 - \frac{\phi^2}{F^2}]^{\frac{1}{2}} \tag{38}$$

and M is related to quark masses. Derivation can be found in [12, 13].

5 Simulations of pion production on thin target

Proton-nucleus collisions are sources of secondary particles which can be further used for high energy physics experiments. A good example is provided by pions, which decay and produce muons and neutrinos. Unfortunately, this subject which is treated by particle and nuclear physics is not easy to handle in detail due to a serious lack of experimental data for full particle spectra and angular distributions, over a large variety of nuclei and kinetic energies. However it is possible to make predictions using Monte Carlo codes which have been tested on existing data.

I decided to compare particle generations from FLUKA'99 [14] and UrQMD [15] in order to estimate the pion collection efficiency for a neutrino factory or a muon collider. I concentrated on the case of proton kinetic energy of 2 GeV and a mercury target, which is the present base line of the CERN neutrino factory project. The energy range is justified, because new channels for particle production open at higher energies, which reduces the pion yield as expressed per GeV and makes the theoretical description of the processes even more complex. I decided to use two independent codes: FLUKA'99 (CERN, Milano) which presents the advantage for simulating thick targets, UrQMD (Ultra- Relativistic Quantum Molecular Dynamics) (Frankfurt) which could provide a better description of physical processes. The only baryonic projectiles allowed in FLUKA are protons or neutrons, whereas UrQMD gives a richer choice, for example, one can test a deuteron beam. The simulation on hydrogen showed that both codes yield similar results to the spectrum and the angular distributions of the pions, as shown in figure 6 and 7.

Single pion production:

$$NN \rightarrow \pi NN$$

has its treshold around 290 MeV in empty space, while pion induced single pion production:
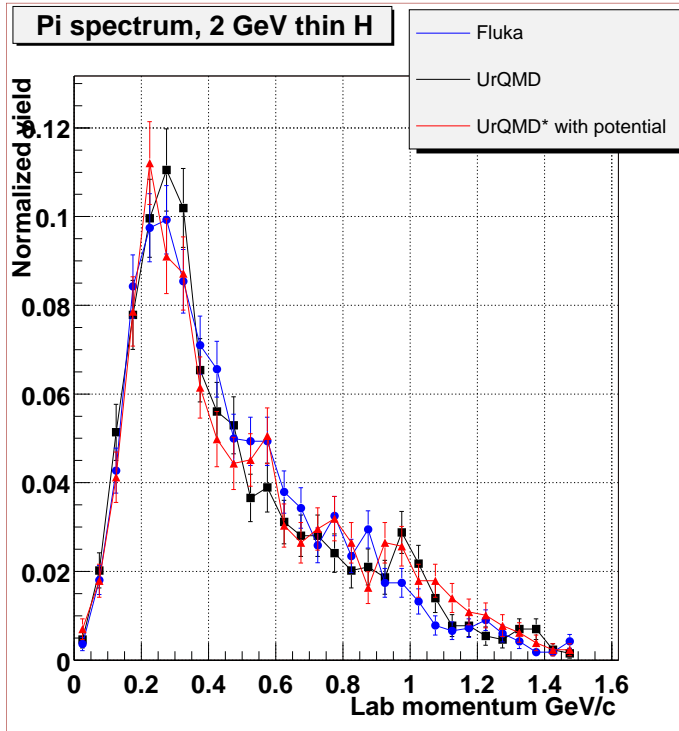
$$\pi N \rightarrow \pi \pi N$$
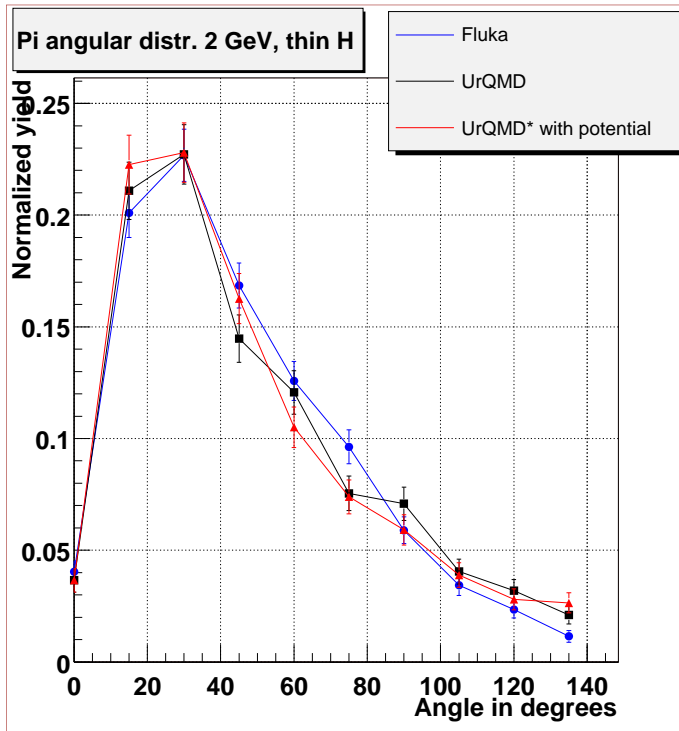
Figure 6: Pion spectrum from hydrogen target.

Figure 7: Pion angular distribution from hydrogen target.

opens at 170 MeV. In both codes pions are mostly produced via

$$\text{NN} \rightarrow \Delta(1232)\text{N} \rightarrow \pi\text{NN}$$

where isospin and charge are conserved. Heavier mesons and baryon species can also participate in pion production, for example:

$$\text{NN} \rightarrow N^*(1440) \rightarrow \pi\text{NN}$$

$$\pi\text{N} \rightarrow N^*(1440) \rightarrow \rho(770)\text{N}\pi\pi\text{N}$$

$$\pi\text{N} \rightarrow \Delta(1600) \rightarrow \pi\Delta(1232) \rightarrow \pi\pi\text{N}$$

$$\pi\text{N} \rightarrow \rho(770)\text{N} \rightarrow \pi\pi\text{N}$$

$$\pi\text{N} \rightarrow \pi\Delta(1232) \rightarrow \pi\pi\text{N}.$$

Pions can also be produced via double pion production, which opens at 600 MeV for nucleon - nucleon scattering:

$$\text{NN} \rightarrow \pi\pi\text{NN}$$

and about 350 MeV for pion - nucleon reaction:

$$\pi\text{N} \rightarrow \pi\pi\pi\text{N}.$$

As examples the following reactions can be taken:

$$\text{NN} \rightarrow \Delta(1232)\Delta(1232) \rightarrow \pi\pi\text{NN}$$

$$\text{NN} \rightarrow \text{N}N^*(1440) \rightarrow \text{N}\pi\Delta(1232) \rightarrow \pi\pi\text{NN}$$

$$\pi\text{N} \rightarrow \Delta(1600) \rightarrow \pi N^*(1440) \rightarrow \pi\pi\Delta(1232) \rightarrow \pi\pi\pi\text{N}$$

$$\pi\text{N} \rightarrow \omega(782)\text{N} \rightarrow \pi\pi\pi\text{N}$$

$$\pi\text{N} \rightarrow \rho(770)\Delta(1232) \rightarrow \pi\pi\pi\text{N}.$$

Many more channels for reactions are possible including the fact, that in medium effective masses can be lower and more species have to be taken into account. In particular in UrQMD, a richer particle spectrum is implemented. In heavy nuclei such as mercury, pions can rescatter inside the nucleus in which they are produced and thus be affected by charge exchange reactions:

$$\pi^+\text{n} \rightarrow \pi^0\text{p}$$

$$\pi^0\text{n} \rightarrow \pi^-\text{p}$$

$$\pi^0\text{p} \rightarrow \pi^+\text{n}$$

$$\pi^-\text{p} \rightarrow \pi^0\text{n}$$

One can anticipate that the cascade details in nucleus play an important role. In a nuclear medium cross sections of the underlying processes can be different from their values in vacuum. This is accounted for in UrQMD through the use of effective masses and particle momenta in nuclear matter. In addition the potential inside nucleus has different terms
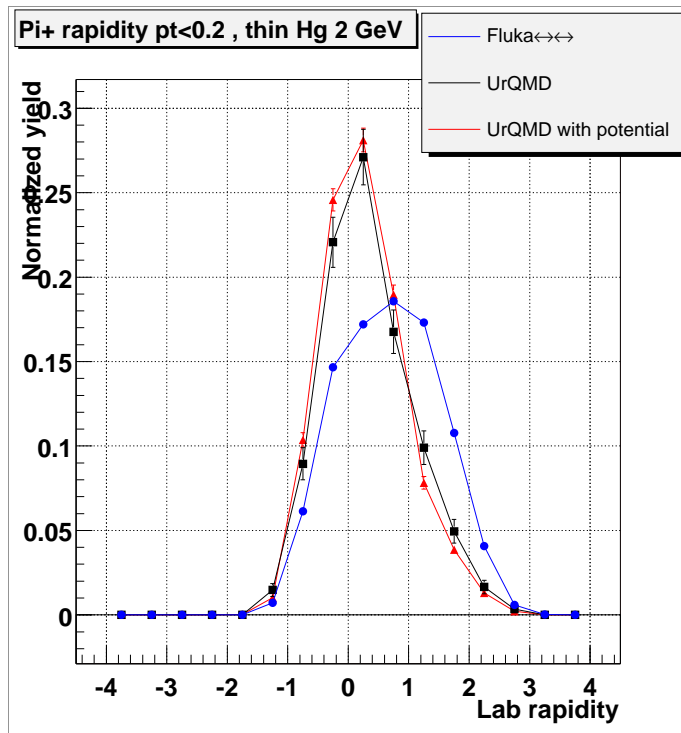
Figure 8: Rapidity plot of π^+ from Hg.

in each code. Both of them turn on the Pauli blocking and sample nucleons in the initial nucleus according to the Fermi momentum and nuclear density.

To test particle generation FLUKA has been run using a thin 1 mm mercury target, which gives a probability of rescattering inside the target on the level of 1%. The same probability of reinteraction was used in the hydrogen target. The thickness of targets was calculated according to hadronic interaction length. The UrQMD has been used with two options: with (UrQMD*) and without a potential. Figures 8, 9, 10, 11, 12 and 13 present comparison of rapidities, spectra and angular distributions for π^+ and π^- separately.

On spectrum plots one can see a maximum, which can be a signature of Δ - particles decaying almost at rest inside a nucleus. There is a difference between curves representing separate simulations. In particular there exists a big difference in altitude of the maximum explained above. It can be understood, that different number of Δ particles decay at rest. The difference in UrQMD runs (with and without potential) can be explained in the following way: potential suppresses some collisions and reduces a degree of relaxation inside a nucleus. Because of that maximum is smaller than in the case of nopotential run. Fluka simulation showed even smaller value. Comparison of angular distributions showed a difference in both codes. UrQMD presents bigger pion production at higher angles to the proton beam line. A comparison of spectrum and angular distribution on hydrogen and mercury thin targets for Fluka and UrQMD separately (see Fig. 16, 17, 18, and 19) is also interesting. Here one can see different results in the case of UrQMD and similar results for Fluka. UrQMD presents different treating of both targets: the spectrum has bigger maximum and angular distribution is wider for mercury in comparison to hydrogen. In the case of Fluka results of hydrogen and mercury runs are similar. Only some rescaling can be seen.
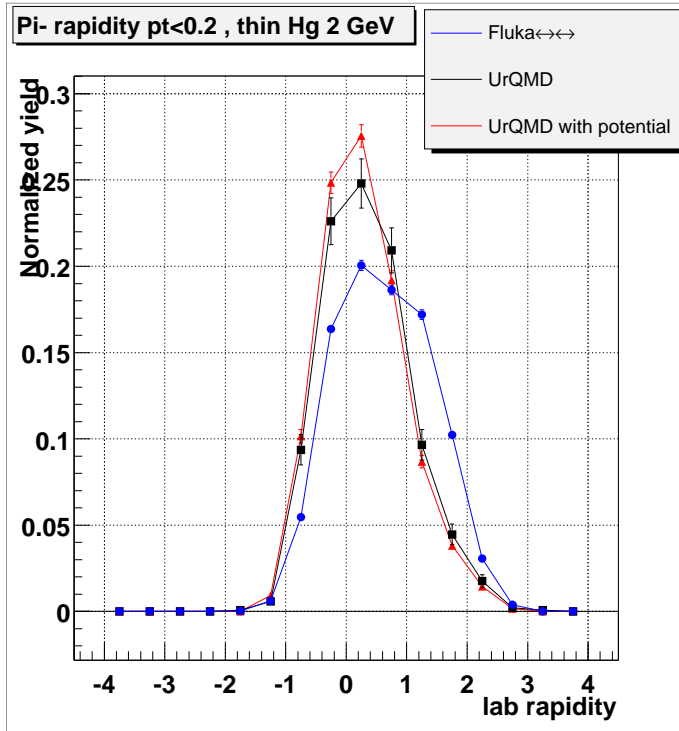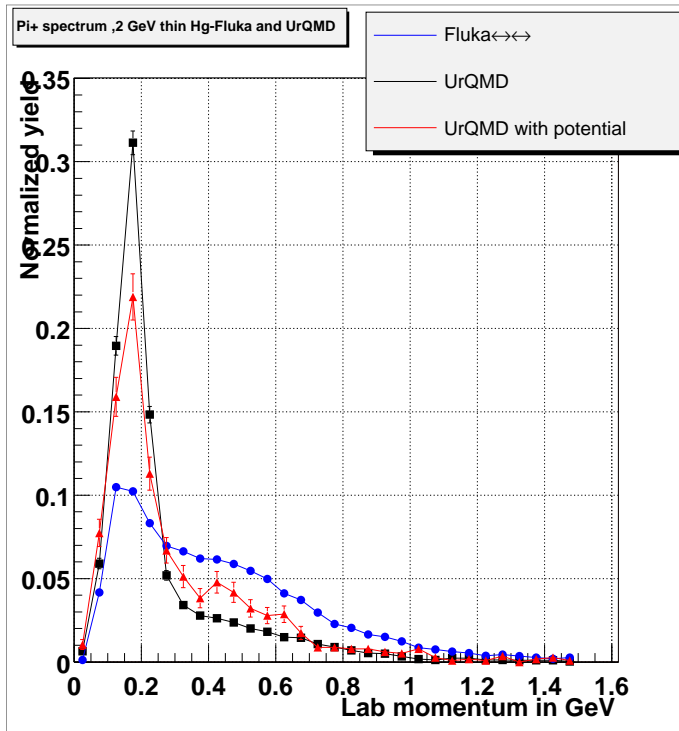
Figure 9: Rapidity plot of π^- from Hg.

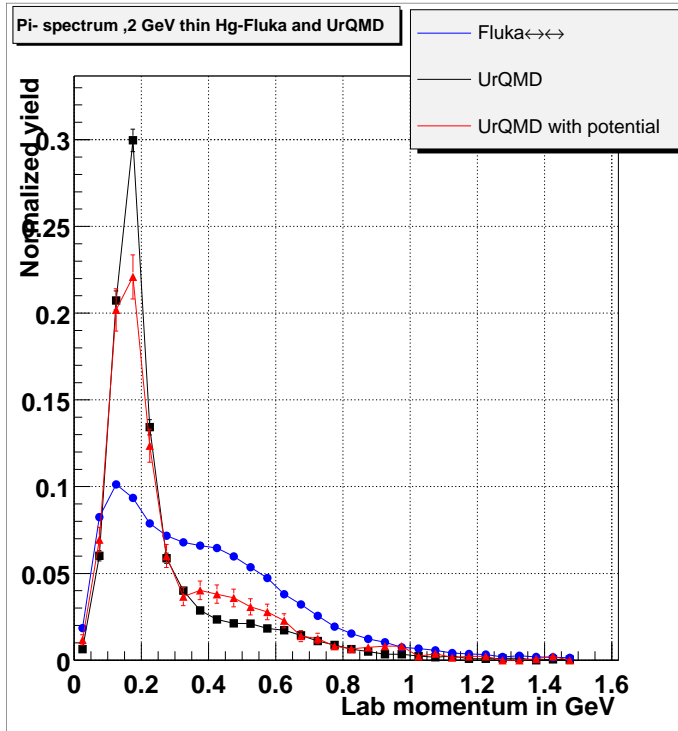Figure 10: π^+ spectrum from Hg.
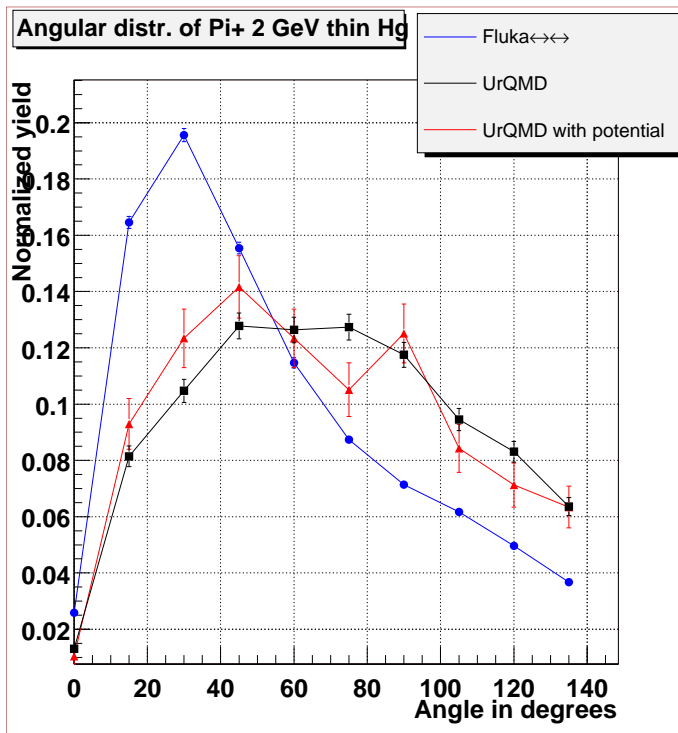
20

Figure 11: π^- spectrum from Hg.

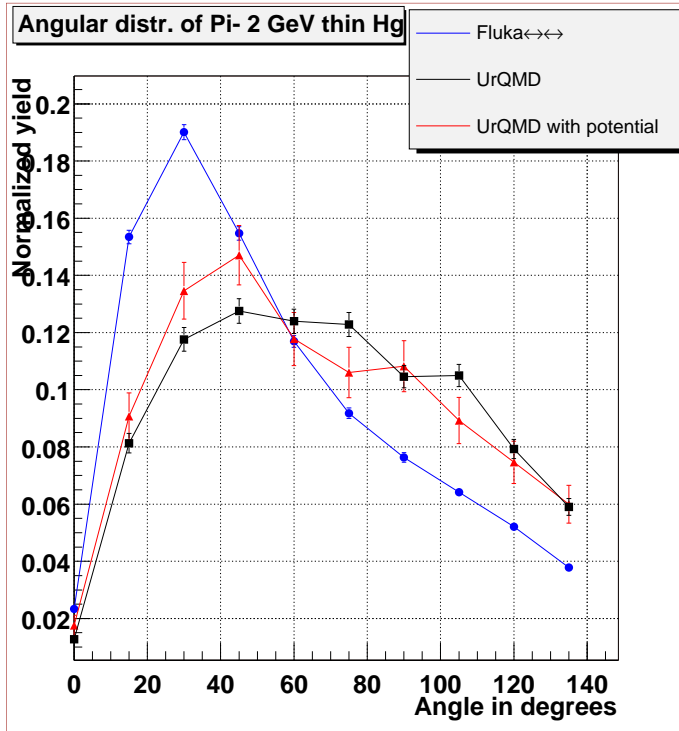Figure 12: π^+ angular distribution from Hg.

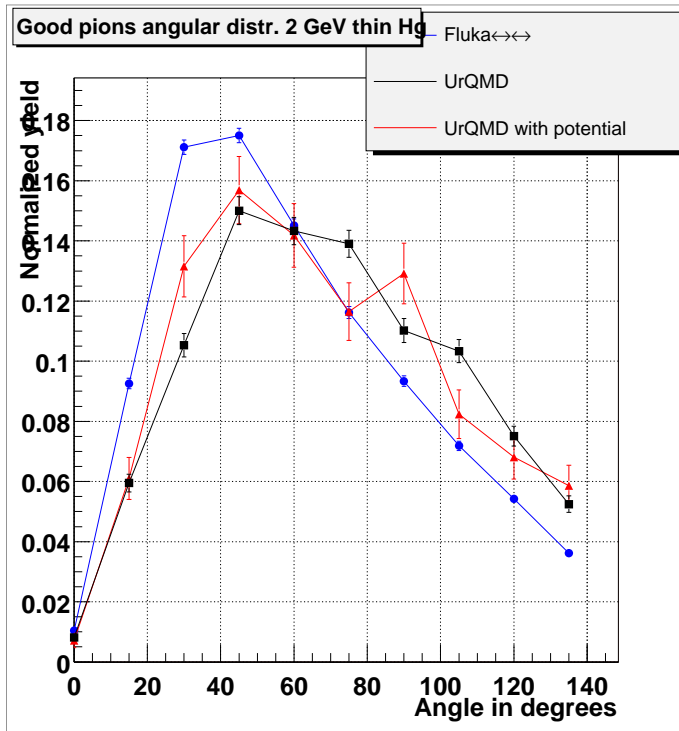Figure 13: π^- angular distribution from Hg.

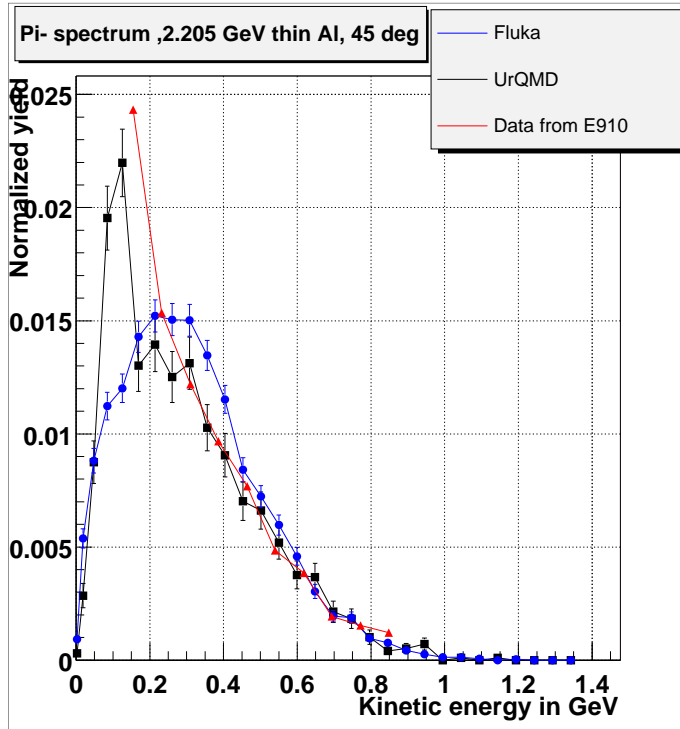Figure 14: Angular distribution of pions from rapidity interval 1-2.

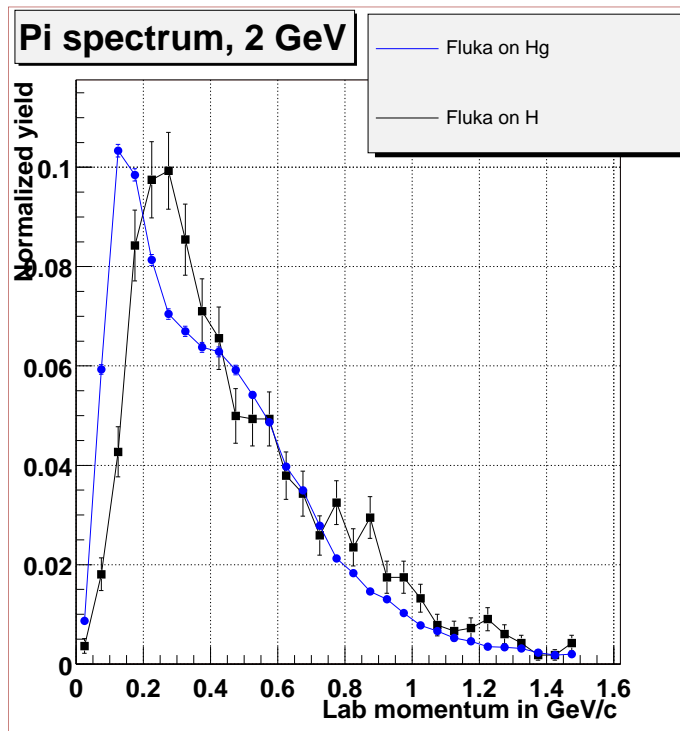Figure 15: Comparison of simulations with E910 data.

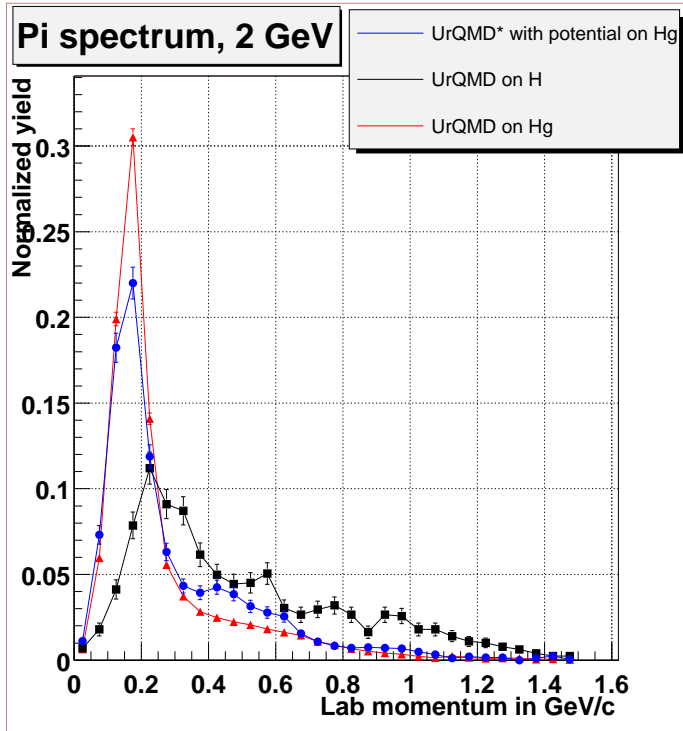Figure 16: π spectrum from Fluka on hydrogen and mercury.

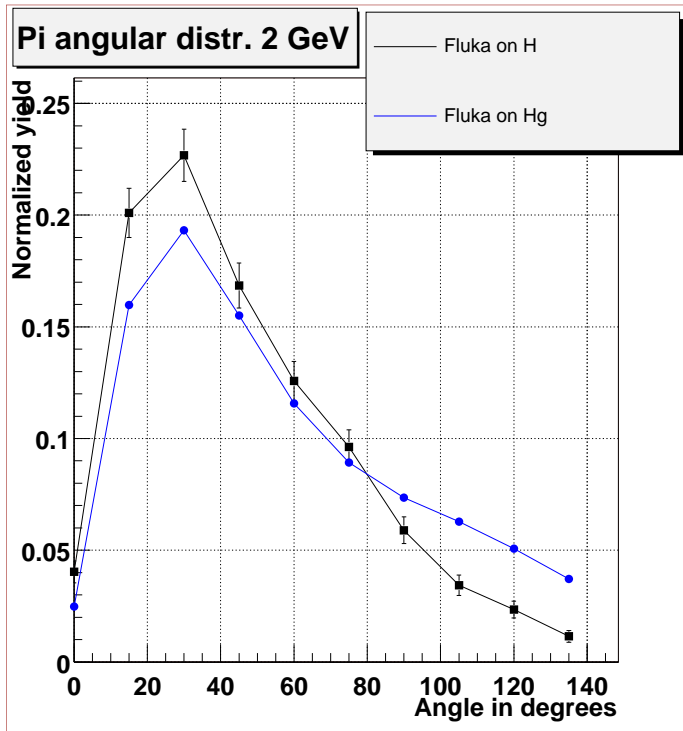Figure 17: π spectrum from UrQMD on hydrogen and mercury.

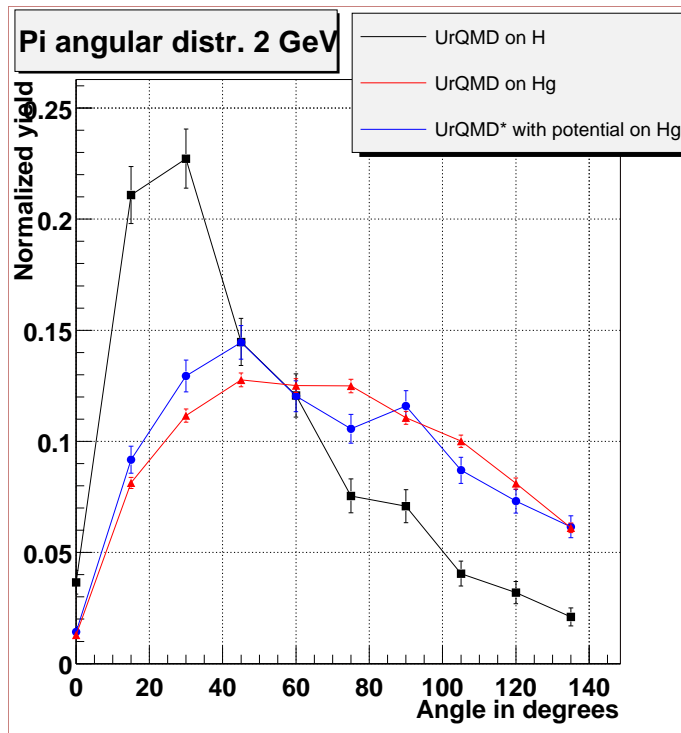Figure 18: π angular distribution from Fluka on hydrogen and mercury.

Figure 19: π angular distribution from UrQMD on hydrogen and mercury.

Table 1 presents comparison of pions produced per proton deposited on target, per inelastic interaction and ratio of positive and negative pions from UrQMD and Fluka. First two quantities were calculated according to fitting to interaction length assumed to be constant (see discussion in chapter 2.) and taking all interactions in UrQMD as inelastic. These assumptions contain big uncertainties. Only π^+/π^- ratio is exact according to production models considered in the codes. Here we find a difference: Fluka produces more π^+ in respect to UrQMD. There exists a big discussion in the nuclear physicists community about it. π^+/π^- ratio is affected by the ratio of protons to neutrons both in the target material and in projectile, but also by charge exchange reactions, which are part of cascade. Behavior of UrQMD from simulation with deuteron as a projectile on mercury target for the same kinetic energy shows further suppresssion of π^+ (ratio π^+/π^- equal 0.6). It is important to note, that simulations at lower kinetic energy (730 MeV protons) on lead target showed that UrQMD reproduces approximately experimental value 1.95 taken from [26], but Fluka gives too many π^+ (π^+/π^- about 2.5).

Name of code	$\pi \times 10^{-3}$/proton	π/inelastic int.	π^+/π^-
Fluka	3.922	0.5118	1.3
UrQMD	5.005	0.6532	0.87
UrQMD with potential	4.821	0.6292	0.84

Table 1. Results of simulations on thin mercury target.

It can be understood, that in this energy range Fluka presents a production model, which takes into account mostly single nucleon - nucleon interaction inside a nucleus and only some rescaling of the results between different nuclei. UrQMD seems to treat cascade inside a nucleus (rescattering and absorption) more seriously. Here a difference between hydrogen and mercury is explicit. In principle one can expect it, but a production model should be experimentaly verified.

I compared our simulations with data from the E910 experiment [16] (with π^- and proton energy of 2.205 GeV), as shown in figure 15. Both codes reproduce approximately this experimental data except in the low energy region where there is almost no experimental data available. The low energy part of spectrum shows a difference between both codes. The rapidity is calculated from: $\mathrm{rap}_z = 1/2 \cdot \log(\frac{p_z + E}{p_z - E})$ and the normalized yield is given from: $\mathrm{NY} = \dfrac{\text{yield per bin}}{\text{total yield}} \cdot (\text{per charge})$

6 Longitudinal versus transverse collection on thick target

For simulation of a thick target only FLUKA was used. From the thin target results one can read, that the angular distribution for pions in the momentum range 164-504 MeV/c (rapidity interval 1-2 with $p_t = 0$) has a maximum at about 40-60 degrees (both codes produce approximately this maximum) - see Fig 14. This feature could be employed to collect pions with several independent channels around the target [17] under some angle to the proton beam line. The table 2 presents a percentage of pions produced in kinematical window (rapidity 1-2 and $p_t < 0.2$ GeV) for different angles to the proton beam line. (Here rapidity is calculated according to given angles.)

Angle	Fluka [%]	UrQMD [%]	UrQMD with potential [%]	Fluka on thick target [%]
90°	16.9	19.0	18.8	15.1
80°	20.6	21.4	21.0	19.2
60°	29.3	25.3	25.7	29.8
40°	34.7	24.2	26.6	36.8
20°	26.1	15.9	17.3	27.7
0°	11.9	6.4	7.1	12.1

Table 2. Percentage of pions produced in kinematical window (rapidity 1-2 and $p_t < 0.2$ GeV) for 64 channels according to given angle (for 0° only 1 channel is assumed).

Figures 20 and 21 explain the geometry of transverse collection. In this case, a target magnetization, which requires a sophisticated solenoid is not needed. The problem with the secondary proton beam is also solved. But a new problem appears, the reunification of several independent beams.
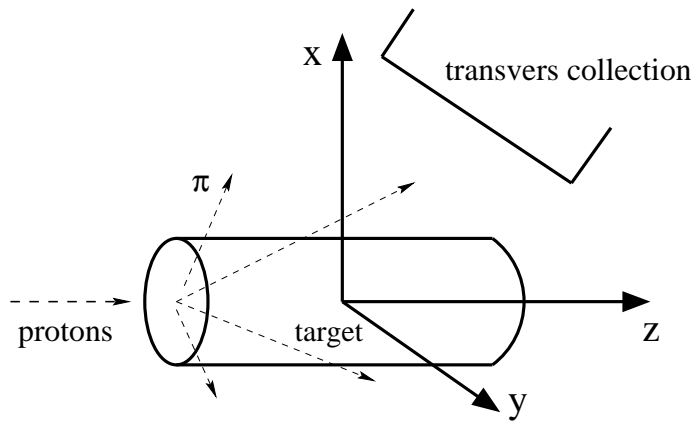
Figure 20: Geometry of transverse collection - view parallel to the proton beam.
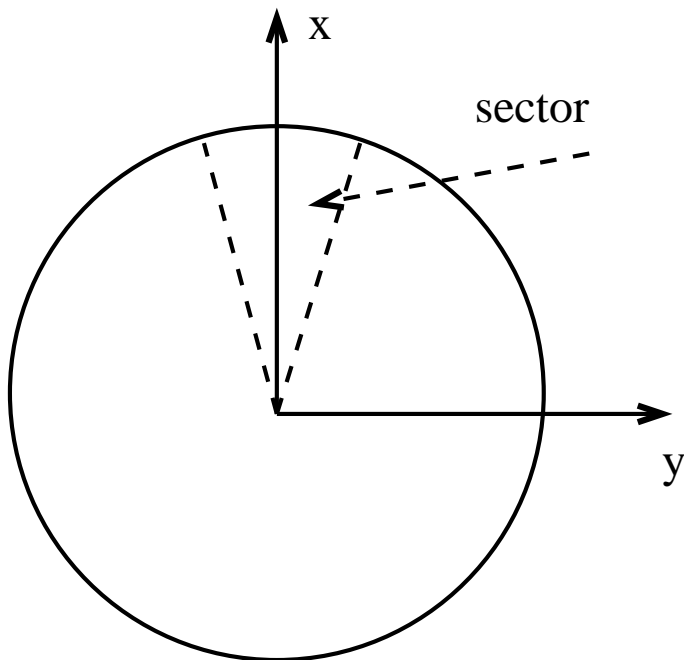

Figure 21: Geometry of transverse collection - view perpendicular to the proton beam.
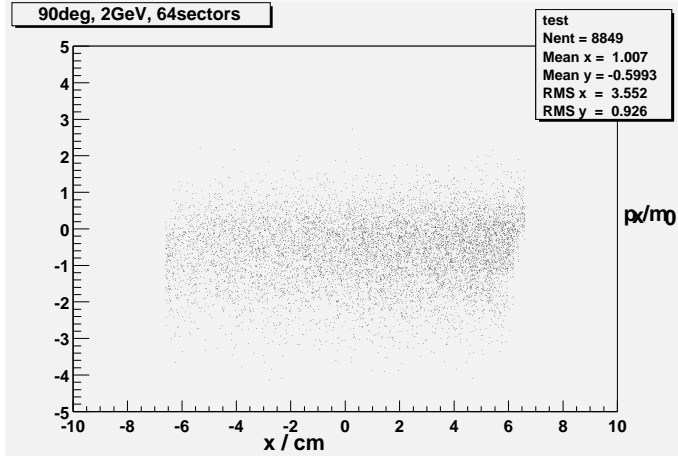
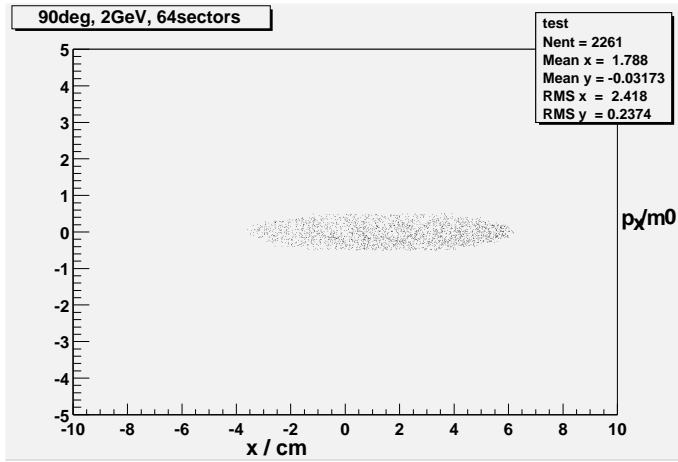Figure 22: Transverse emittance plot for π in (p_x,x) plane.

Figure 23: Transverse emittance for π - (p_x,x) plot with cutoff.

I considered the idea to use of resistive quadrupoles with a normalized emittance 6 $\times$ 10^{-3} m.rad and superconducting ones with an normalized emittance of 24 $\times$ 10^{-3} m.rad. I examined the use of 16 and 64 quadrupoles placed around the target at angles 45 and 90 degrees. I considered 4 MW proton beam power. The transverse emittance plots in (x, p_x) and (y, p_y) planes are shown on Fig. 22 and 24. (Note a change of coordinates: z is now beam axis of quadrupole and x is along the target.) Then cutoff for emittance is applied according to given values. It can be seen as elipses introduced in emittance plots (Fig. 23 and 25). Table 3 presents comparison of calculated number of pions collected per second for different angles and for given number of collecting channels to longitudinal collection in 20 T selenoid and 20 cm target (calculated by J. Collot [27]).
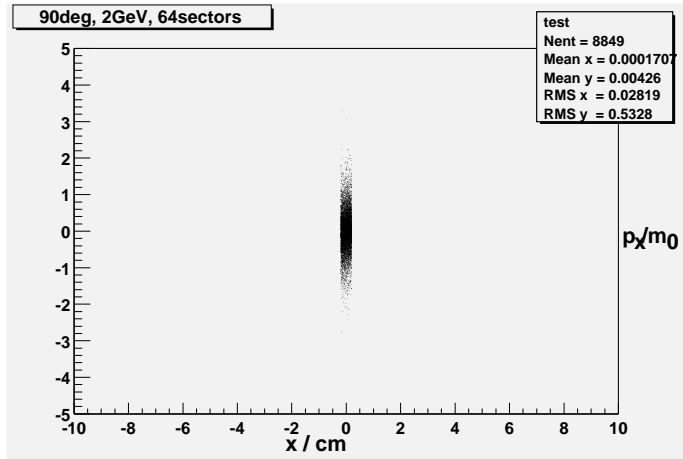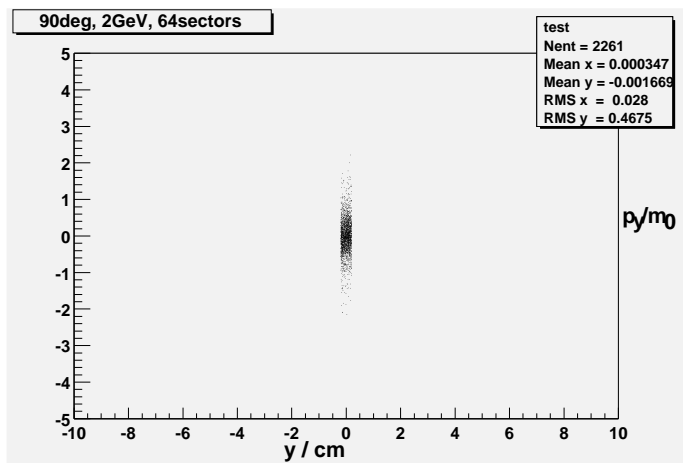
Figure 24: Transverse emittance plot for π in (p_y,y) plane.

Figure 25: Transverse emittance for π - (p_y,y) plot with cutoff

Number of sections	$\varepsilon[m.rad]$	$\theta[°]$	$\pi^+ \times 10^{13}/s$	$\pi^- \times 10^{13}/s$
16	$6 \cdot 10^{-3}$	45	4.2	2.9
		90	1.0	0.9
	$24 \cdot 10^{-3}$	45	16	11
		90	4.1	2.7
64	$6 \cdot 10^{-3}$	45	9.2	7.2
		90	3.5	2.6
	$24 \cdot 10^{-3}$	45	31.0	25.0
		90	10.0	8.0
1 (longitudinal collection)	$24 \cdot 10^{-3}$	0	8.3	5.1

Table 3.Comparison of transverse collection according to given angle and number of collecting channels with longitudinal collection for 20 T selenoid and 20 cm long target.

My tests of particle generation show that Monte Carlo codes produce different results in the region where there exists no experimental data. The need of an experiment to verify the models is obvious. There is a hope that the HARP experiment at CERN and E915 in Fermilab will help to solve this problem. The results show that a large number of pions can be detected in transverse directions. For longitudinal collection a big p_t acceptance is needed, but one might study the transverse collection as an alternative.

7   Transport in nuclear matter

Knowledge of physics in nuclear matter is one of the most fundamental subjects, giving employment for physicists. There are plenty reasons for it: most of the matter which exists in Earth is contained in nuclei, conditions in nuclear matter govern a behavior of neutron stars but also nucleosynthesis played a major role even in creation of life. To test physics in nuclear matter people make heavy ion collisions (HIC) in different energy ranges. The most fascinating experiments are to deal with quark qluon plasma (QGP), which is a topic, where theoretical predictions are very difficult. This year CERN released an information about discovery of QGP in fix target experiments using 33 TeV lead beam on lead target (about 156 AGeV in the center of mass).

Unfortunately there exists presently no theoretical model that provides consistent understanding of the dynamics of heavy ion collisions over the whole energy range. In every energy range different methods are used. At low energy it is sufficient to introduce hadronic species, which are treated as fundamental ones. At higher energy building blocks of hadrons: quarks and gluons have to be taken into account in parton scattering or hadronic string excitation and fragmentation. To describe it people created simulation codes, which turn on and off several models depending of scenerio and also enable to work in cases, where other methods cannot overcome a many body problem. We are interested in proton-nucleus collisions with 2 GeV proton kinetic energy. In this range parton model cannot be used. Asymptotic freedom makes the QCD coupling constant small and makes the pQCD applicable only at higher energy. It allows to treat quarks and gluons approximately like a free point particles - partons.

Now I will describe how simulation codes work. I will treat the UrQMD as a well described example in literature, but I will also try to make some comments about Fluka. In low energy simulations are organized in the following way:
- Nucleons in initial nucleus are represented by Gaussian shaped density distribution:

$$\phi_j(x_j, t) = (\frac{2\alpha}{\pi})^{\frac{3}{4}} exp[-\alpha(x_j - r_j(t))^2 + \frac{i}{\hbar}p_j(t)x_j] \tag{39}$$

- Initial nucleus satisfies the following constrains:

$$\sum_i r_i(0) = 0 \tag{40}$$

what means that it is centered in configuration space around 0,

$$\sum_i p_i(0) = 0 \tag{41}$$

and is at rest.
- The nucleus radius is equal:

$$R \sim r_0 A^{\frac{1}{3}} \tag{42}$$

- Nucleons are sampled according to Bethe - Weizsäcker density and between 0 and Thomas - Fermi momentum:

$$p_F^{max} = \hbar c(3\pi^2\rho)^{\frac{1}{3}} \tag{43}$$

Now we meet a problem how to propagate nucleons in nuclei and incorporate collisions and production of new particles. There are several different ways to do it. In a first approximation particles are moving freely between collisions - this is commonly called cascade. When their distance is small enough:

$$d \leq \sqrt{\frac{\sigma_{tot}}{\pi}} \tag{44}$$

two particles collide and cross section has to be incorporated into the code. In the next step potential inside nucleus should be taken into account and the fact that some of the particles inside nucleus (mostly nucleons) obey Fermi statistics and have to be subject to Pauli blocking. There are many models to incorporate this. One can use well known potentials like Yukawa, Coulomb , but also density dependent interactions like Skyrme two and three body interaction:

$$V^{Sk} = t_1 \sum_{i<j} \delta(x_i - x_j) + t_2 \sum_{i<j<k} \delta(x_i - x_j)\delta(x_i - x_k) \tag{45}$$

or some parametrizatitons of a potential (mean field) like the following one with density dependence:

$$V(\rho) = A(\frac{\rho}{\rho_0}) + B(\frac{\rho}{\rho_0})^\sigma \tag{46}$$

where $\sigma > 1$, A is attractive and B repulsive. A mean field approch can incorporate momentum dependence:

$$V(\rho, p) = V_v\rho + \frac{V_s\rho}{\sqrt{1 + \frac{p}{m}}}. \tag{47}$$

In general potential should be momentum, density, spin, isospin dependent and can be a very complicated expression. Apriori it could be possible to extract the potential from assumed interaction Lagrangian and such a possibility is studied.

There are two methods to include the Pauli principle. The first one is to introduce a potential, which looks like:

$$V_P = V_P^0 (\frac{\hbar}{q_0 p_0})^3 exp[-\frac{|r_i - r_j|^2}{2q_0^2} - \frac{|p_i - p_j|^2}{2p_0^2}]\delta_{\sigma_i \sigma_j}\delta_{\tau_i \tau_j} \qquad (48)$$

where σ_i and τ_i represent spin and isospin of i particle. The second way is to make a cluster decomposition in the phase space and define a density f(r,p,t)=n/N of a species, where N is maximal number of particles of a given type in a cluster. Then collision takes place when a distance condition is satisfied and when final-state phase space factor:

$$[1 - f(r, p_1, t)][1 - f(r, p_2; t)] > x, \qquad (49)$$

where x is a random number in the interval between 0 and 1. This condition is also a very good example to see how Monte Carlo simulations work.

When a collision is allowed by above two condition a cross sections is turned on, which in general has a form:

$$\sigma_{12 \to 34}(\sqrt{s}) = (2S_3 + 1)(2S_4 + 1)\frac{<p_{34}>}{<p_{12}>(\sqrt{s})^2}|M(m_3, m_4)|^2 \qquad (50)$$

If outgoing particles are stable, momentum in the center of mass can be described by the formula:

$$<p_{34}>(\sqrt{s}) = p_{CMS}(\sqrt{s}) = \frac{1}{2\sqrt{s}}\sqrt{(s - (m_3 + m_4)^2)(s - (m_3 - m_4)^2)} \qquad (51)$$

($<p_{12}>$ is defined as above by exchanging m_3, m_4 with m_1, m_2 respectively). However if outgoing particles are not stable but resonances the width of their mass distribution must be incorporated. Than the formula (51) has to be modified to:

$$<p_{34}>(\sqrt{s}) = \int \int p_{CMS}(\sqrt{s}, m_3, m_4)A_3 A_4 dm_3 dm_4 \qquad (52)$$

where the integration is done between threshold for resonance production and maximum available energy. A is a Breit-Wigner distribution:

$$A_r(m) = \frac{1}{2\pi}\frac{\Gamma}{(m_r - m)^2 + \frac{\Gamma^2}{4}} \qquad (53)$$

The matrix elements are parametrized to fit experimental data or if there is no data available estimated by some theoretical considerations. For example for $\Delta_{1232}(3,3)$ production:

$$NN \to N\Delta_{1232}$$

a matrix element has a form:

$$|M(\sqrt{s}, m_3, m_4)|^2 = A\frac{m_\Delta^2 \Gamma_\Delta^2}{((\sqrt{s})^2 - m_\Delta^2)^2 + m_\Delta^2 \Gamma_\Delta^2} \qquad (54)$$

Unstable particles can decay according to their branching ratios and life times. Here a full power of Monte Carlo method is used.

Here we arrive at the problem if cross sections or decay widths in nuclear medium are the same as in vaacum. It seems that they are not and some corections should be introduced. I will try to tell few words about it a little later.

Particles propagation between collisions is governed by classical equation of motion - this feature seemed very strange for me at the beginning, but as I will try to show it can be justified on the quantum level. First of all until now nobody could solve the many body problem and to get some results people try to omit the problem in some ways.

I will make a short ansatz to quantum transport theory in its nonrelativistic version [18, 19]. Let's define commutation relation for fields in Heisenberg picture:

$$\hat{\Psi}(\vec{x}, t)\hat{\Psi}^\dagger(\vec{y}, t) \pm \hat{\Psi}^\dagger(\vec{y}, t)\hat{\Psi}(\vec{x}, t) = \delta^3(\vec{x} - \vec{y})$$

$$\hat{\Psi}(\vec{x}, t)\hat{\Psi}(\vec{y}, t) \pm \hat{\Psi}(\vec{y}, t)\hat{\Psi}(\vec{x}, t) = 0 \tag{55}$$

where upper sign refer to fermionic field and lower to bosonic one. Let's define a Green function - one particle propagator:

$$iG(X, Y) = < 0|T(\Psi(X)\Psi^\dagger(Y))|0 > \tag{56}$$

where T is a time ordering operation. It enables description of particle propagation in equilibrium. For non-equilibrium situations this formula is no longer valid. In this case we cannot make identification of asymptotic states, it means that states at $t \to +\infty$ cannot be (like in equilibrium) identified with the states at $t \to -\infty$ modulo a phase factor. This identification is lost because of irreversibility. In that case time ordering should be treated independenly for increasing and decreasing time. We define Green functions:

$$g^c(1, 1') = \theta(t_1 - t_1')g^>(1, 1') + \theta(t_1' - t_1)g^<(1, 1')$$

$$g^a(1, 1') = \theta(t_1' - t_1)g^>(1, 1') + \theta(t_1 - t_1')g^<(1, 1')$$

$$g^-(1, 1') = g^<(1, 1') - g^a(1, 1') = g^c(1, 1') - g^>(1, 1')$$

$$g^+(1, 1') = g^>(1, 1') - g^a(1, 1') = g^c(1, 1') - g^<(1, 1') \tag{57}$$

where:
$$\pm ig^<(1, 1') = < \hat{\Psi}^\dagger(1')\hat{\Psi}(1) >$$

$$\pm ig^>(1, 1') = < \hat{\Psi}(1)\hat{\Psi}^\dagger(1') > \tag{58}$$

θ is the Heaviside function and c,a,- and + stay for causal, anticausal, advanced and retarded Green functions. Here the symbol $<>$ means expectation value with some state or trace with the density operator. Let's note that expression

$$\pm ig^<(1, 1) = n(1) \tag{59}$$

can be interpreted as spatial density of particles.

The Fourier tranformation in relative variables of such density constitutes the so-called Wigner function in phase-space:

$$f(p, R, T) = \int dr e^{-ipr} < \hat{\Psi}^\dagger(R - r/2, T)\hat{\Psi}(R + r/2, T) > \tag{60}$$

33

Figure 26: Time contour from definition of time path ordered Green functions.

where $r = x_1 - x_2$, $t = t_1 - t_2$, $R = (x_1 + x_2)/2$, $T = (t_1 + t_2)/2$. It can be generalized to be also a distribution in energy. Explicit formula can be written in the following way:

$$\pm i g^<(p, \omega, R, T) = \int dr \int dt e^{-ipr+i\omega t}(\pm)i g^<(r, t, R, T) \tag{61}$$

Here:

$$g^<(r, t, R, T) \equiv g^<(x_1, t_1, x_2, t_2) \tag{62}$$

Now the distribution function can be written:

$$f(p, R, T) = \int \frac{d\omega}{2\pi}(\pm i) g^<(p, \omega, R, T) \tag{63}$$

It is important to note that from commutation relations (55) we have:

$$i(g^> \pm g^<)(\vec{r}, t, \vec{r'}, t) = \delta(\vec{r} - \vec{r'}) \tag{64}$$

and consequently:

$$\int \frac{d\omega}{2\pi}(\pm i) g^>(p, \omega, R, T) = 1 \pm f(p, R, T) \tag{65}$$

Interaction Hamiltonian in the nonrelativistic situation can be taken as:

$$\mathcal{H} = \int d\vec{r} \Psi^\dagger(X) \frac{\nabla^2}{2m} \Psi(X) + \frac{1}{2} d\vec{r} d\vec{r'} \Psi^\dagger(X) \Psi^\dagger(X') V(|\vec{r} - \vec{r'}|) \Psi(X') \Psi(X). \tag{66}$$

In the relativistic case we could introduce covariant Lagrangian or Hamiltonian density like Lagrangian of QHD (see equation 34) or chiral perturbation theory (see equation 35).

It is convenient to introduce time path ordered Green functions in the following way: we redefine time ordering operation which orders operators lying on a contour placed along a path axis (see fig. 26), which goes from $t = -\infty$ to $t_{max}(\to +\infty)$ and back to $-\infty$ by a different path. In this way we define a causal and anticausal ordering replacing all operators from antychronological branch to the left of operators from the chronological branch.

Now we can make a perturbation expansion similar to the conventional Feynman graph technic. We can define a generalized Dyson equation:

$$iG(1, 1') = iG_0(1, 1') + \int_C d2' d2 G_0(1, 2') \Pi(2, 2') iG(2', 1'), \tag{67}$$

where G denotes generalized Green function which can be c, a, < or >, $\int_C$ means integration along the time contour and G_0 denotes free propagator. It can be also a definition of a self energy Π, which is very important quantity in the transport theory and is sometimes called optical potential. Self energy can be split in three parts according to the formula:

$$\Pi(X, Y) = \Pi_{MF}(X)\delta'(x, y) + \Pi^>\Theta(t_x, t_y) + \Pi^<\Theta(t_y, t_x), \tag{68}$$

where Θ is time ordering along a contour and δ' is a generalized Dirac delta, which equals zero for arguments from different branches and is standard Dirac delta up to the sign for the same time branch (minus for lower branch). Using relation for Schrödinger operator and free propagator:

$$(i\partial_t + \frac{\nabla^2}{2m})G_0(1,1') = -\delta(1,1') \tag{69}$$

we obtain the Kadanoff and Baym equations [20]:

$$[i\partial_{t_1} + \frac{\nabla_1^2}{2m} - \Pi_{MF}(1)]G^<(1,1') = \int d2[\Pi^+(1,2) + G^<(2,1') + \Pi^<(1,2)G^-(2,1')],$$

$$[i\partial_{t_{1'}} + \frac{\nabla_{1'}^2}{2m} - \Pi_{MF}(1')]G^<(1,1') = \int d2[G^+(1,2)\Pi^<(2,1') + G^<(1,2)\Pi^-(2,1')] \tag{70}$$

and similar for other functions.

Now I present some motivation for VUU equation (Vlasov-Uehling-Uhlenbeck) also called BUU equation (Boltzmann-Uehling-Uhlenbeck). It is not a full derivation but some arguments concerning it. The transport equations are derived assuming weak dependence of Green functions G(1,1') and self energies $\Pi(1,1')$ on the sums of arguments and that they are significantly different from zero only when the differences of arguments are close to zero. Let's introduce convenient variables:

$$G(X,u) \equiv G(X - \frac{1}{2}u, X + \frac{1}{2}u) \tag{71}$$

Assume that G(X,u) and Π(X,u) vary slowly with X and are strongly peaked for u≅0. Due to this assumption one can introduce so called gradient expansion:

$$G(X + u, u) \cong G(X,u) + u^i \frac{\partial}{\partial X^i} G(X,u) \tag{72}$$

which is useful to perform the Wigner transformation. After aplication of the Wigner transformation to Kadanoff-Baym equations and subtracting these equations one finds:

$$i(\frac{\partial}{\partial T} + \frac{p}{m}\nabla R - \nabla R\Pi_{MF}\nabla p)G^<(\omega,p,R,T) = \Pi^>(\omega,p,R,T)G^<(\omega,p,R,T)$$

$$-\Pi^<(\omega,p,R,T)G^>(\omega,p,R,T) \tag{73}$$

The self energy can be evaluated using perturbative expansion. The lowest order terms is Hartree-Fock energy:

$$\Pi^1(1,1') = \delta'(t_1,t_{1'})[\delta(x_1 - x_{1'})\int dx_2 V(x_1 - X_2)(\pm i)G^{0<}(x_2,t_1,x_1,t_1)$$

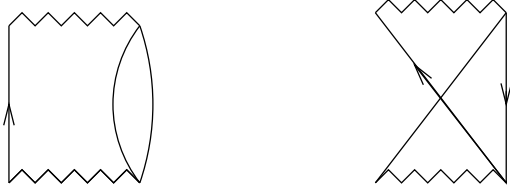$$+V(x_1 - x_{1'})iG^{0<}(x_1,t_1,x_{1'},t_1)] \tag{74}$$

Figure 27: Lowest order diagrams (up) and Born diagrams (down) for self energy.

The Born direct and exchange terms are of particular interes for us, they look like:

$$\Pi_{Bd}^< = \pm \int \int dx_2 dx_{2'} V(x_1 - x_2) V(x_{2'} - x_{1'}) G^<(1,1') G^<(x_2, t_1, x_{2'}, t_{1'}) G^>(x_{2'}, t_{1'}, x_2, t_1)$$

$$\Pi_{Be}^< = - \int \int dx_2 dx_{2'} V(x_1 - x_2) V(x_{2'} - x_{1'}) G^<(1, x_{2'}, t_{1'}) G^<(x_2, t_1, 1') G^>(x_{2'}, t_{1'}, x_2, t_1) \quad (75)$$

To derive the final equation a quasiparticle approximation is introduced, which takes into account only particles on mass shell. In this approximation most of higher order terms in self energy are dropped. It introduces an energy delta function and enable to write:

$$\pm i G^<(\omega, p, R, T) = Z(p, R, T) 2\pi \delta(\omega - \omega_p) f(p, R, T) \quad (76)$$

where $\omega_p = \frac{p^2}{2m}$ and

$$Z^{-1}(p, R, T) = 1 - \frac{\partial Re \Pi^(\omega, p, R, T)}{\partial \omega}|_{\omega = \omega_p} \quad (77)$$

It is important to note, that in relativistic theory [21, 22, 23] which is a covariant formulation of transport theory where the derivation is similar, the quasipartical approximation is a method to introduce medium effects with a help of effective masses and momenta for particles. The argument of effective mass goes as follows: after summation in Dyson expansion Green function can be written:

$$G(X, P) = [P^2 - m_\pi^2 - \Pi_M(X) - i\epsilon]^{-1}. \quad (78)$$

Effective mass for pion is defined via:

$$m_\pi^{*2} = m_\pi^2 + \Pi_M \tag{79}$$

where self energy is in quasiparticle approximation.

Now I will come back to nonrelativistic case and write transport equation. Taking into account only Born terms on the right side of equation (73), applying Wigner transformation to the last ones (75), taking into account quasiparticle approximation (76) and using formulas (63) and (64) after some calculations we can obtain the VUU (BUU) equation:

$$(\frac{\partial}{\partial T} + \frac{p}{m}\nabla_R - \nabla_R U(R,T)\nabla_p)f_A(p,R,T) =$$

$$= \frac{4}{(2\pi)^3} \sum_{B,C,D} \int dp_1 dp_2 dp_3 d\Omega |v_{12}| \frac{d\sigma_{(A+B\to C+D)}}{d\Omega}\delta(p + p_1 - p_2 - p_3)$$

$$[f_C(p_2,R,T)f_D(p_3,R,t)(1 \pm f_A(p,R,T))(1 \pm f_B(p_1,R,T))$$

$$- f_A(p,R,T)f_B(p_1,R,T)(1 \pm f_C(p_2,R,T))(1 \pm f_D(p_3,R,T))] \tag{80}$$

Distribution functions $f_W(p,R,T)$ (W represents here A, B, C or D) can refer to different particles, for example pions, nucleons or deltas. Sign + in parenthesis on the right side of the VUU equation corresponds to bosons and - to fermions. In a realistic situation we have a set of coupled equations for distribution functions, but analytical solution does not exist. However it is possible to use the molecular dynamics and Monte-Carlo methods. The test particles method [24] is used to solve a problem: we approximate distribution function by an ensamble of test particles and to keep contact with a particle interpretation to each particle corresponds $\tilde{N}$ test particles. Test particles move classically between collisions according to Hamilton's equations:

$$\dot{P}_i = -\nabla_R U(\rho(R_i))$$
$$\dot{R}_i = v_i \tag{81}$$

Here v_i can be treated relativistically and U(R) can be calculated in a framework of a chosen model or put by hand. Test particles can collide and a cross section for it is taken as $\frac{\sigma}{\tilde{N}}$. If colliding test particles represent fermions, Pauli blocking should be respected. In collisions two test particles change from $(R_1, P_1)(R_2, P_2)$ to $(R_1, P_1')(R_2, P_2')$. We build spheres in phase-space around (R_1, P_1') and (R_2, P_2') such that n test particles imply complete filling of volume ($n = \tilde{N}N$, where N is a number of real particles, which fill the sphere). Define $f_1 = \frac{n1}{n-1}$ where n_1 is the number of test particles in a phase-space volume without the test particle at (R_1, P_1'). Doing similar for f_2 we can apply Monte-Carlo method in the usual way calculating a probability of scattering $(1 - f_1)(1 - f_2)$. Using test particles method in collision with inelastic interactions we meet problems with interpretation of causality of collision. For example it is possible that two test particles which could represent the same

nucleon create a pion. There is a discussion how to treat this problem. Some people take $\tilde{N} = 1$ and get QMD or UrQMD-like models. In the VUU approach we use quantum physics in derivation of this equation. We make quasiparticle approximation taking only particles on-shell, gradient expansion and include only Born terms in collisions. It can be questioned in particular in the case of pion propagation in nuclear medium (it is possible, that better description of pion absorption is taken into account by reactions with more than one nucleon-absorption via deuteron formations in nucleus). But we preserve a quantum behavior of a system in a potential, in collisions and definition of distribution function, which should be understand in a statistical way so that the Heisenberg principle of uncertainty is not broken. Classical equations of motion appear only in simulations, while the distribution function has a quantum character. However authors of UrQMD use a variational approch to justify classical equation in as deep quantum system as nucleus is, it can be interpreted in the way explained above.

8 Conclusions

Simulations showed explicitly that experimental verification of physical model to predict hadronic yields at kinetic energy of order 10^1 GeV is very important. In collecting scenario for the neutrino factory or the muon collider bigger p_t acceptance beyond 0.2 GeV is needed and in particular a collector with low longitudinal cutoff should be built to incorporate the low energy maximum of yield. Here magnetic horn may be used as a solution, but one can also consider a superconducting selenoid or a transverse collection in several quadrupoles around the target. Present quantum transport theory approach needs further development to understand approximations used and to go beyond their limitations. Also the way of solving transport equations should be studied both from theoretical and numerical point of view.

References

[1] R. N. Mohapatra and P. B. Pal, "Massive neutrinos in physics and astrophysics", second edition, World Scientific 1991.

[2] C. W. Kim and A. Pevsner, "Neutrinos in physics and astrophysics", Contemporary Concepts in Physics Nr 8, 1993.

[3] S. Geer, Phys. Rev. D 57, 6989, (1998).

[4] B. Autin, "Technical challanges of neutrino factories", CERN 1999.

[5] D. M. Kaplan, "Muon Collider / Neutrino Factory: Status and Prospects, physics/0001037.

[6] D. Neuffer, "$\mu^+ - \mu^-$ Colliders", CERN 99-12.

[7] J. F. Gunion, "Physics Motivations for Muon Collider", hep-ph/9605396.

[8] B. Autin, A. Blondel and J. Ellis eds., "Perspective Study of Muon Storage Rings at CERN", CERN 99-02.

[9] S. Humphries, "Charged particle beams", Wiley 1990.

[10] T. Ericson and W. Weise, "Pions and Nuclei", International Series of Monographs on Physics, Clarendon Press 1988.

[11] B. D. Serot and J. D. Walecka Adv. Nucl. Phys. 16, 1 (1986).

[12] S. Weinberg, "The Quantum Theory of Fields", vol. 2: modern applications, Cambridge University Press 1996.

[13] Chiral dynamics: theory and experiment, Workshop on Chiral Dynamics - Mainz'97, Lecture Notes in Physics Nr 513, Springer - Verlag 1998.

[14] A. Ferrari and P. R. Sala, "The Physics of High Energy Reactions", in Proceedings of the Workshop: Nuclear Reaction Data, Design and Safety, Miramare - Trieste'96.

[15] S. A. Bass at al.,Prog. Part. Nucl. Phys. 41, 255 (1998).

[16] J. Collot, H. G. Kirk and N. V. Mokhov, "Pion Production Models and Neutrino Factories", Talk at NuFact'99 in Lyon.

[17] B. Autin and Ph. Royer, "Transvers Collection of Pions", CERN 1999.

[18] P. Danielewicz Annals of Physics 152, 239 (1984).

[19] C. Grégoire, "Introduction to non relativistic transport theories", Les Houches Winter School in Theoretical Physics'89.

[20] L. P. Kadanoff and G. Baym, "Quantum Statistical Mechanics", Benjamin 1962.

[21] S. Mrówczyński and P. Danielewicz, Nucl. Phys. B 342, 345 (1990).

[22] W. Botermans and R. Malfliet, Phys. Rep. 198, 115 (1990).

[23] Guangjun Mao, L. Neise, H. Stöcker and W. Greiner, Phys. Rev. C 59 Nr 3, 1674 (1999).

[24] G.F. Bertsch and S. das Gupta, Phys. Rep. 160, 189 (1988).

[25] D. E. Groom at al. Europ. Phys.J. C15, 1 (2000).

[26] M.M. Sternheim and R. R. Silbar, Phys. Rev. D 6, 3117 (1972).

[27] J. Collot - private communication, see also talk on NuFact'99 conference by J. Collot, H. Kirk and N. Mokhov http://lyoinfo.in2p3.fr/nufact99.